A THEORETICAL MODEL FOR LIPID MIXTURES, PHASE TRANSITIONS, AND PHASE DIAGRAMS

H. L. SCOTT AND WOOD-HI CHENG, *Department of Physics, Oklahoma State University, Stillwater, Oklahoma 74074 U.S.A.*

ABSTRACT We present a new model for the thermodynamic properties of lipid bilayers. The model consists of a system of hard cylinders of varying radii that correspond to the different molecular radii of lipids having different numbers of gauche rotations in their chains. Scaled particle theory is used to provide an accurate estimate of the entropy of packing of the cylinders. To apply the model to bilayers we introduce a semiempirical attractive potential energy. Once the form of this potential is chosen, we adjust one parameter, the interaction strength, so that the model fits the transition temperatures and entropies for various phospholipids. The model then agrees quite well with other published data for these systems. We also directly generalize our model to lipid mixtures, and we obtain phase diagrams that we compare to existing data for these systems. We use the model to describe lipid protein interactions in bilayers as well.

I. INTRODUCTION

In this paper we present a new model for the thermal properties of lipid monolayers and bilayers. The model differs from those presented recently by other authors (Nagle, 1973, 1976; Marčelja, 1974; McCammon and Deutch, 1975; Jackson, 1976), but is similar in part to the model of Scott (1975) and in part to the model of Jacobs et al. (1975). The major goal of this work is to present a reliable model for single-component lipid bilayer phase transitions observed in the homologous series of 1,2-diacylphosphatidyl cholines (DMPC,[1] DPPC, DSPC, DBPC) using an accurate description of lipid packing and a semiempirically constructed potential energy function. An advantage of this model is that it is readily generalized from a single-component to a multicomponent system. In section II we describe the model and its application to pure systems. In section III we generalize the model to two-component systems. Section IV gives the results of our analysis, and section V presents our conclusions.

II. THE MODEL

The experimental properties of lipid in monolayers and bilayers provide several hints for the development of new models. For example, the rather large mobility of lipids within the plane

[1] *Abbreviations used:* DMPC dimyristoylphosphatidylcholine; DPPC, dipalmitoylphosphatidylcholine; DSPC, distearoylphosphatidylcholine; and DBPC, dibehenoilphosphatidylcholine.

Dr. Cheng's present address is Telecommunications Laboratories, Ministry of Communications, P. O. Box 71, Chung-Li, Taiwan, Republic of China.

of a monolayer (Devaux and McConnell, 1972) suggests that relatively little entanglement of chains between molecules occurs. This, together with an almost constant order parameter over most of the chains (Seelig and Niederberger, 1974) suggests a model in which gauche bonds occur largely in pairs, forming kinks or jogs that can move rapidly up and down a chain. This would imply that rapidly rotating lipid molecules with these rapidly moving kinks can be treated approximately as cylinders whose radius is proportional to the number of kinks. Another consequence of this reasoning is that only a finite number of allowed radii for the cylinders need be considered, and the many possible states of lipid molecules in either monolayer of a lipid bilayer may be classified by sets of cylinders of varying area. Then the thermodynamic state of the system depends upon a set of quantities $\{\alpha_i\}$ that denote the fraction of molecules in the various cylinder states. Since many different isomeric states have approximately the same area there are relatively few cylinder states to count, although each state may be formed in many ways by a large variety of chain conformations.

If the cylinders are infinitely hard, then the packing of different states of lipid molecules in a two-dimensional layer is identical to the packing of a two-dimensional mixture of hard disks. A technique that seems to work well in the description of such hard disk systems is scaled particle theory (Lebowitz et al., 1965). The method is based upon an estimate of the work required to add a single hard-disk to the system, and the resulting thermodynamic properties are remarkably consistent with other analytical theories (Frisch and Lebowitz, 1964) and computer simulations (Alder and Wainwright, 1960) of hard-core systems in one, two, and three dimensions.

From scaled particle theory the equation of state and chemical potential for a mixture of hard disks are given, respectively, by

$$\beta P = \left[\frac{\Sigma \rho_i}{(1 - \pi\Sigma \rho_i R_i^2)}\right] + \left[\frac{\pi(\Sigma \rho_i R_i)^2}{(1 - \pi \sum_i \rho_i R_i^2)^2}\right] \tag{1}$$

$$\beta\mu_i = kT \ln\left[\rho_i \frac{h^3}{(2\pi m_i kT)^{3/2}}\right] + \left[-\ln(1 - \pi\Sigma \rho_i R_i^2) + \left(\frac{2\pi(\Sigma \rho_i R_i) R_i}{(1 - \pi\Sigma \rho_i R_i^2)}\right) + \beta\pi\rho R_i^2\right], \tag{2}$$

where P is the pressure, μ_i is the chemical potential of the i species, ρ_i and R_i are the density and radius of a particle of the i species, respectively, and β is the reciprocal of the absolute temperature times Boltzmann's constant.

From Eqs. 1 and 2 we can rewrite the Helmholtz free energy of a mixture of hard disks as a function of T, A, A_i, and α_i, where A is the total area, A_i the molecular area of cylinders in state i, and α_i is the fraction of particles in state i. Beginning with

$$F_{HC} = \sum_i N_i\mu_i - PA = (A/\beta)(\beta\Sigma\rho_i\mu_i - \beta P), \tag{3}$$

we form F_{HC}, the hard-core free energy, from Eqs. 1 and 2. The entropy of packing is then given by

$$S = Nk\left[1 - \Sigma\alpha_i \ln \alpha_i + \ln\left(\frac{A}{N} - \sum_i \alpha_i A_i\right) - \frac{(\Sigma \alpha_i \sqrt{A_i})^2}{\left(\frac{A}{N} - \sum_i \alpha_i A_i\right)}\right]. \quad (4)$$

We turn now to the manner in which our model treats rotational isomerism in lipid systems. As mentioned earlier, order parameter studies suggest that in the upper regions of closely packed chains pairwise kinks or jogs that leave the chains parallel to each other are the best disordering mechanism. In the formation of one kink, two *trans* configurations in the CH_2 chain are transformed into gauche configurations and the chain is shortened by one CH_2 unit of length. We also allow jog states of the form (g ... *TT* .. *g*), discussed by Seelig and Niederberger, which may also move up and down the chain. By formation of one jog, the chain is shortened by n CH_2 lengths, where n is the (odd) number of *trans* segments between the two gauche segments. In all cases where these pairwise conformations occur the radius of the molecule is increased by an amount proportional to the amount by which the chain shortens. Let us take DMPC as an example. There are 13 bonds per chain for DMPC (C_{14}) and we consider only 11 of these units as rotatable (we exclude the top and last units). We suggest six possible classes of configurations for C_{14}, including from 0–6 rotations per chain. To compensate for not explicitly including all possible states assign weights W_i, determined by combinational arguments as in Scott and Cheng (1977), to each state. In Table I various chain states, weights W_i, and average number of gauche rotations in each state are listed. For example, for state 3 for DMPC we group together all states with chains shortened by two CH_2 units. Denumerating all possible ways this can occur in a double chain molecule, we find 192 distinct states. Of these, 160 contain four gauche rotations, 16 contain three, and 16 contain two. Thus, the mean number of gauche rotations for this state is 3.75.

By similar reasoning, we have developed a 7-state model for DPPC, an 8-state model for DSPC, and a 10-state model for DBPC. The various chain states, degeneracies, and average number of gauche rotations in each state are given in Table I. Now we must assign area A_i to

TABLE I
PROPERTIES OF MODEL STATES FOR THE SYSTEMS UNDER CONSIDERATION

State No.	DMPC			DPPC			DSPC			DBPC		
	W_i	A_i	g_i	W_i	A_i	g_i	W_i	A_i	g_i	W_i	A_i	G_i
		Å²			Å²			Å²			Å²	
1	1	40.8	0	1	—	0	1	—	0	1	—	0
2	20	43.9	2	24	43.5	2	28	43.2	2	36	42.7	2
3	192	47.6	3.75	280	46.6	3.79	384	45.9	3.81	1,612	44.9	3.94
4	676	51.9	5.84	1,328	50.2	5.90	5,240	48.9	5.97	5,460	47.2	5.96
5	192	57.1	4.75	328	54.4	4.78	9,456	42.5	7.83	33,184	49.9	7.91
6	20	63.5	4	256	59.3	4.84	1,116	56.5	5.42	132,580	52.8	9.83
7	—	—	—	24	65.2	4.50	728	61.2	4.58	3,684	56.1	6.96
8	—	—	—	—	—	—	28	66.8	5.00	4,660	59.8	6.16
9	—	—	—	—	—	—	—	—	—	1,312	64.1	6.93
10	—	—	—	—	—	—	—	—	—	36	69.0	6.00

W_i is the statistical weight assigned by combinatorial analysis, and g_i is the weighted average number of gauche rotations in each state. A_i is the area associated with state i, from Eq. 5.

the various states in the model. Experiments show that the volume change accompanying the bilayer phase transition is <5% (Nagle and Wilkinson, 1978). From this fact it seems reasonable to neglect this ΔV, as a first approximation for the chain structures and write the average areas as functions of chain length:

$$A_i L_i = A_o L_o. \tag{5}$$

Here L_o is the length of a hydrocarbon chain in the all-*trans* conformation with an average cross-sectional area A_o = 20.4 Å^2 (Tardieu et al., 1973). A_i and L_i are the effective cross-sectional area and length of given configuration i, respectively. Thus, 40.8 Å^2 represents the minimum hard-core area of a molecule. This is not to be confused with A, the thermodynamic average area per molecule used later. The approximation of Eq. 5 was also used by Marčelja (1974), and yields the hard-disk areas for the states of Table I.

The treatment described in the previous paragraphs gives us a simple accurate treatment of the hard-core packing problem in conjunction with the rotational isomeric model in a two-dimensional lipid monolayer (each half of a bilayer is considered independent). It is much more difficult to construct a theoretical model for which the long-range attractive forces are treated accurately. As discussed by Nagle (1973) a most reasonable approximation is to consider the bilayer to be a continuum and to obtain the intermolecular attractive energy by integrating the potential over the two-dimensional area. This procedure yields the result

$$E_{\text{att}} = -C/A^{3/2}, \tag{6}$$

where A is the molecular area and C is the interaction strength. If we consider only nearest neighbor interactions, the exponent in Eq. 6 becomes 5/2 but this does not appreciably change the properties of the model. Studies of the properties of this model, using Eq. 6 for E_{att}, reveal that no phase transitions occur for reasonable values of C at physiological temperatures. This results because we assume infinitely hard cores in our packing calculation. We are, therefore, led to modify Eq. 6 and construct a semiempirical potential energy function. In so doing, we strive to keep our function as physically realistic as possible and to avoid arbitrary introduction of parameters. The simplest correction to Eq. 6 that should compensate for the overly strong hard-core interactions is to replace the molecular area A by $(A - A_0)$, where A_0 is a constant less than the minimum possible value of A. This gives us the potential

$$E_{\text{att}} = -\frac{C}{(A - A_0)^{1.5}}. \tag{7}$$

A_0 is a constant to be determined in Eq. 7. We shall avoid using A_0 as a fitting constant, however, and simply set A_0 = 38 Å^2 in all subsequent computations for lipids. This value seems reasonable because it is less than the minimum molecular area, 40.8 Å^2, so that no singularity is involved and the potential energy varies more rapidly near the close packing limit than does Eq. 6. The only remaining adjustable quantity in the semiempirical potential is the constant C. With C chosen for each phospholipid so that the model agrees with experimental results, we have in Eq. 7 a reliable phenomenological potential for use with the scaled particle treatment. We then test the predictive abilities of the model by considering lipid-lipid and lipid-protein mixtures. Our potential is certainly not unique, but we feel that

the manner in which Eq. 7 was chosen is physically consistent with the actual bilayers we study.

We now combine our results to form the Helmholtz free energy of half of a lipid bilayer of DMPC, according to the equation $F = F_{rot} + E_{att} + F_{HC}$:

$$F/NKT = \frac{500}{RT}\left(\sum_{i=1}^{6} g_i\alpha_i\right) - \frac{C_{(14)}}{RT(A-38)^{1.5}} - \left\{1 - \sum_{i=1}^{6}\alpha_i \ln(\alpha_i/W_i) + \ln\left(A - \sum_{i=1}^{6}\alpha_i A_i\right) - \frac{\left(\sum_{i=1}^{6}\alpha_i\sqrt{A}\right)^2}{\left(A - \sum_{i=1}^{6}\alpha_i A_i\right)}\right\}. \quad (8)$$

The first term, E_{rot}, is the energy of gauche rotamers, obtained using 500 cal/m as the energy of *trans*→gauche excitation, and using the effective number of gauche bonds per state given in Table I. All the summations in this equation are over all the various states of DMPC. The parameters g_i, W_i, and A_i are determined from Table I. Similarly, we can obtain the free energies of the other members of the homologous series. The summations in these free energies go over all various seven, eight, and ten states for DPPC, DSPC, and DBPC, respectively.

For computation of bilayer properties we minimize the Gibbs free energy, $G = F + \pi A$, with respect to the α_i and A at fixed temperature and surface pressure π. For the computation of monolayer properties we find the values of the α_i that minimize the Helmholtz free energy at fixed temperature and area. The minimization program used is the routine STEPT (written by J. P. Chandler, Computer Science Department, Oklahoma State University). Location of minima in or near two phase regions required careful approaches to the points of interest in thermodynamic space. Incorrect approaches often resulted in only one of two phases being found consistently. The best approach seemed to be to start out at very high temperatures to locate the fluid-like phase or at very low temperatures to lcoate the solid-like phase, and gradually let T approach the desired temperatures from above or below, respectively. The phase transitions in single-component systems may be analyzed in either of two ways. For bilayers, the procedure described in the previous paragraph produces two sets of values for G, one for a high area (fluid-like) phase and one for a low area (solid-like) phase. Plots of these quantities versus temperature give two curves, G(fluid) and G(solid). The physical state is always associated with the smallest value of G so that, where the curves cross, the system changes phase. In our studies of bilayers the $\pi - A$ term in the Gibbs free energy produces lower molecular area, since this term decreases with A. An identical effect could be achieved by using a larger van der Waals constant C and no $\pi - A$ term. However, we feel that our approach is more realistic in that there should be an interfacial energy at the bilayer surface that contributes to the free energy in the same fashion as a $\pi - A$ term. To select the proper value of π, we use the guideline suggested by Hui et al. (1975) and Nagle (1976), $\pi = 50$ dyn/cm. These workers argue that this pressure is required on a monolayer film to produce bilayer-like packing, so, by extension, in bilayers one should expect a similar effective pressure on the hydrocarbon region, albeit from different physical sources. Marčelja (1974) uses smaller lateral pressures in his models, but in a different physical context. For studies of

monolayers we minimize the Helmholtz free energy with respect to the α_i at fixed A and generate pressure-area isotherms by differentiating F with respect to A.

The analysis of our computations is illustrated in Figs. 1–3. In Fig. 1 one can see that plots of the Gibbs free energy G versus T can be obtained for both a condensed and an expanded phase, characterized, respectively, by low and high molecular areas. The curves cross and keeping G at a minimum implies that the crossing point locates a first-order phase transition. Fig. 2 shows how the transition temperature varies with pressure, and in Fig. 3 we plot the $\pi - A$ properties of the model. In this case one locates the phase transition by performing a Maxwell equal-area construction on the van der Waals loops that occur in the isotherms. Detailed results will be summarized later, and we now describe the computational procedure for binary mixtures.

III. APPLICATION TO BINARY MIXTURES

The theoretical model for pure lipid phase transitions is only the first step towards understanding the structural properties of biological membranes. The effects of molecular heterogeneity in naturally occurring membranes can be studied in model systems such as lipid-lipid or lipid-protein mixtures. There are currently two theoretical models concerned with phase diagrams in binary mixtures of lipid (McCammon and Deutch, 1975; Jacobs et al., 1977). The model of Jacobs et al. (1977) at this time provides the more detailed description of binary lipid mixtures. A major advantage of our approach is that mixtures are directly treated

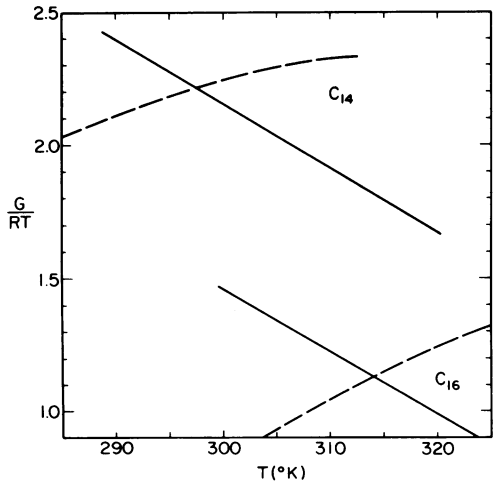

FIGURE 1

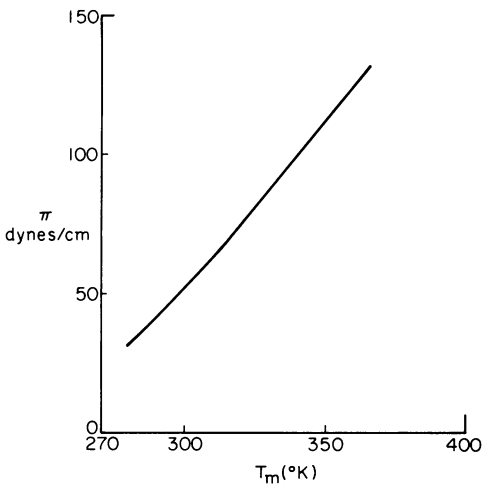

FIGURE 2

FIGURE 1 A plot of Gibbs free energy vs. temperature for DMPC and DPPC layers at fixed lateral pressure of 50 dyn/cm. In each case one curve represents an expanded phase and one a condensed phase. The intersection points, therefore, locate first-order phase transitions.

FIGURE 2 Effect of changes in the effective lateral pressure π on transition temperature for DMPC. The van der Waals-like nature of the semiempirical potential dictates the existence of a critical point, albeit at very high pressure and temperature, as shown. $T_c \simeq 366°K$. $\pi_c \approx 132$ dyn/cm.

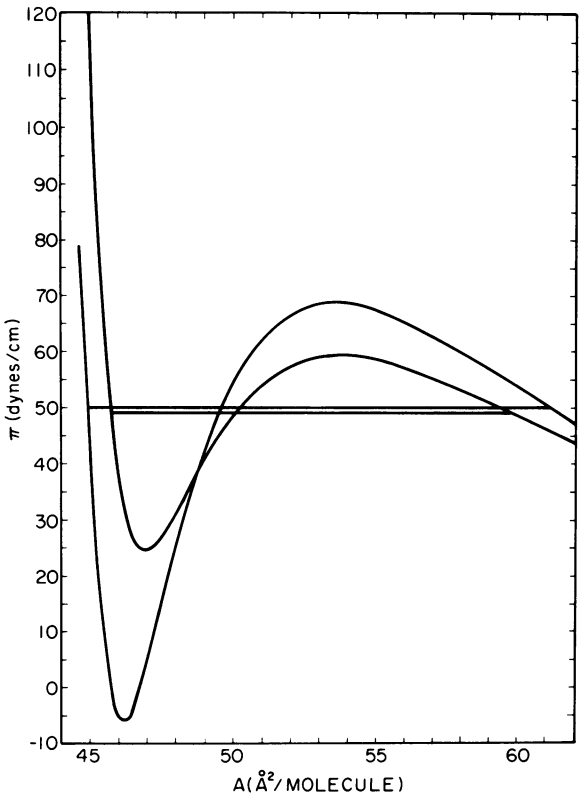

FIGURE 3 Pressure-area isotherms for DMPC and DPPC at 297 and 314°K, respectively. The DMPC isotherm has the smaller loops. The model parameter C is adjusted so that the phase transition at ~50 dyn/cm shown here and in Fig. 1 agrees with the experimental data.

as follows. Consider a binary system with the components denoted by A and B. System A contains N_A molecules and B contains N_B molecules. Let relative concentration of A be X_A and of B be X_B. Molecules A or B may be lipid of different species, or one of the components may be protein or cholesterol. Our technique is applicable as long as both species may be treated as cylinders or groups of cylinders of known radii. Let us first analyze a binary mixture of two lipids, both members of the same homologous series. As before, we consider the lipid molecules to be a mixture of hard disks such that the total number of states is the sum $N_S = N_{A,S} + N_{B,S}$. Here $N_{A,S}$ and $N_{B,S}$ are the number states of component A and B, respectively, used in the single-component systems described in the previous section. Then the packing entropy of the mixture is given by

$$S/NK = 1 - \sum_{i-1}^{N_S} \alpha_i \ln (\alpha_i/W_i) + \ln\left(A - \sum_{i-1}^{N_S} \alpha_i A_i\right) - \frac{\left(\sum_{i-1}^{N_S} \alpha \sqrt{A_i}\right)^2}{A - \sum_{i-1}^{N_S} \alpha_i A_i} - X_A \ln X_A - X_B \ln X_B \quad (9)$$

where

$$X_A = \sum_{i-1}^{k} \alpha_i$$

$$X_B = 1 - X_A = \sum_{i-k+1}^{N_S} \alpha_i.$$

If we assume ideal mixing, so that the average potential at any given molecular site is not dependent upon whether the neighboring molecules are of type A or B, then the attractive energy is simply the weighted sum

$$E_{\text{att}} = -\frac{C(A)X_A + C(B)X_B}{(A - 38)^{1.5}}. \tag{10}$$

$C(A)$ and $C(B)$ are the van der Waals energy constants for the respective one-component systems as determined from the previous section.

As an example, the total free energy of two-component bilayers for C_{14}–C_{16} lipid mixtures is given by

$$G/RT = \frac{500}{RT}\left(\sum_{i-1}^{13} g_i\alpha_i\right) + E_{\text{att}} - \left(1 - \sum_{i-1}^{13} \alpha_i \ln(\alpha_i/W_i) + \ln\left(A - \sum_{i-1}^{13} \alpha_i A_i\right) - \frac{\left(\sum_{i-1}^{13} \alpha_1 \sqrt{A}\right)^2}{A - \sum_{i-1}^{13} \alpha_i A_i}\right) + X_{14} \ln X_{14} + X_{16} \ln X_{16} + \pi A/RT. \tag{11}$$

The summations in this equation from one to seven correspond to C_{16} states and from eight to thirteen correspond to C_{14} states. Here X_{16}, the fixed C_{16} concentration, equals $\Sigma\alpha_i$ over all states of C_{16} molecules, and X_{14}, fixed by $X_{14} + X_{16} = 1$, equals $\Sigma\alpha_i$ over all states of C_{14} molecules. As before, the parameters g_i, W_i, and A_i are determined from our considerations of single-component systems. Similarly, we can obtain the free energies of $C_{14} - C_{18}$, and $C_{16} - C_{18}$, respectively.

For the computation of phase diagrams, we minimize the Gibbs free energy at $\pi = 50$ dyn/cm and values of T between the two systems' transition temperatures. A typical result is shown in Fig. 4. The curves for the solid-like and fluid-like states now cross in a cusp. Thermodynamic considerations dictate that G must be concave, opening upward on the graph. To preserve this concavity, one constructs a line tangent to both curves as shown in Fig. 4. This line then connects the two coexisting phases at the given temperature, and, by varying T, a phase diagram is obtained.

Our basic model may also be readily generalized to mixtures of dissimilar objects, such as lipid and protein or cholesterol. If the predominant interaction between the lipid and the other member of the mixture is hydrophobic, and if little or no strong or orientational interactions are involved, then our approach should be useful. As an example, we consider a mixture of DPPC and a hydrophobic polypeptide, gramicidin A. To apply our model to this mixture, we use the 7-state DPPC model described earlier and add an eighth state, a cylinder of area A_8 that corresponds to the protein's hydrophobic cross section. For gramicidin A we choose A_8 =

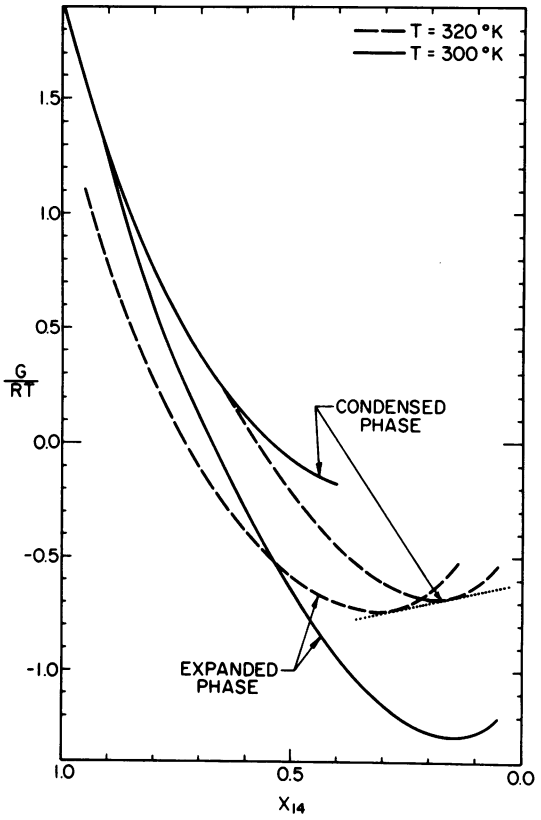

FIGURE 4 Plots of Gibbs free energy vs. concentration for DMPC-DSPC binary mixtures held at π = 50 dyn/cm, at temperatures 320 and 300°K. For each temperature there are two curves, corresponding to expanded and condensed phases. The curves cross in a cusp, and thermodynamic stability then dictates that the cusp must be replaced by the double tangent line that connects coexisting phases, as shown by the dotted line for T = 320°K. The locus of double tangent points for different temperatures defines the phase diagram.

110 Å^2, from the results of Chapman et al. (1977), and we choose a soft-core area for this molecule of A_{soft} = 105 Å^2. As in the single-species case, the soft-core area used in the van der Waals energy prevents a singularity from occurring for physical values of the molecular area. The results of our calculations are sensitive to the value of A_{soft} used (Cheng, 1978). The Helmholtz free energy for this system is

$$F/NkT = \frac{500}{RT}\left(\sum_{i-1}^{8} g_i\alpha_i\right) - \frac{C(16)}{RT[A - (38X_{16} + 105X_{pr})]^{1.5}} - \left\{1 - \sum_{i-1}^{8}\alpha_i \ln(\alpha_i A_i) + \ln\left(A - \sum_{i-1}^{8}\alpha_i A_i\right) - \frac{\left(\sum_{i-1}^{8}\alpha_i\sqrt{A}\right)^2}{A - \sum_{i-1}^{8}\alpha_i A_i}\right\}. \quad (12)$$

The summation from one to seven in this equation corresponds to the model for the C_{16} system and state number of eight corresponds to the protein. Because the dimension of the

protein molecule is greater than that of a lipid molecule, we chose for the protein parameters, $g_8 = 0$, and $W_8 = 1$. The $38X_{16} + 105X_{pr}$ is the minimum (close-packed) area of the hard-core system.

IV. RESULTS

Single-Component Systems

Typical results of our computations for single-component systems are shown in Figs. 1–3. For the four lecithins under consideration the fitting procedure used was to find the value of the parameter C in Eq. 7 for which the bilayer phase transition occurs at the experimental temperature and pressure (taken as ~50 dyn/cm). The values of van der Waals energies at closest packing, $E = C/(40.8 - 38)^{1.5}$, we obtain after the fitting procedure are 0.88, 0.88, 0.88, and 0.85 kcal/mol CH_2 for 14, 16, 18, and 22 carbon chains, respectively and C increases nearly linearly with the number of carbons. These values are smaller than the 1.84 kcal/mol CH_2 sublimation energy for polymethylene, and compare favorably with monolayer cohesive energies measured by Gershfeld (1968). In the fitting procedure it is possible to vary the surface pressure π used in the Gibbs free energy, as well as the interaction parameter C, and in Fig. 2 we show the effects of varying π. There are no completely reliable guidelines currently available for the choice of this effective surface pressure other than monolayer-bilayer comparisons in which the monolayer pressures required to produce bilayer-like packing at temperatures above the bilayer transition temperature are estimated. To our knowledge, the best estimate is based on the experimental studies of Hui et al. (1975) and the theoretical argument of Nagle (1976), both of which suggest $\pi \approx 50$ dyn/cm. We, therefore, use this value exclusively, keeping in mind that lower values of π can still be accommodated if we use larger values of the parameters C. However, as shown in Table II the present choice produces values for the change in van der Waals energies at the transitions that agree remarkably well with the experimental values (Nagle and Wilkinson, 1978). In Fig. 2 the effects of changing π are shown. For lower values of π the T_m is lowered and the entropy change increases. One could fit some of the experimental data with this model by using a smaller π and correspondingly larger values for the constants C. However, we find the phase

TABLE II
EXPERIMENTAL AND CALCULATED PHASE TRANSITION PROPERTIES* OF PHOSPHATIDYLCHOLINES

Lipid	Acyl chain length	Transition temperature	H		ΔU (attractive)	
			Exp.	Calc.	Exp.	Calc.
		K		*cal/mol*		*kcal/mol*
DMPC	C_{14}	297‡	5.4‡	6.2	0.148‖	0.150
DPPC	C_{16}	314‡	8.7‡	8.6	0.171‖	0.180
DSPC	C_{18}	328‡	10.6‡	11.7	0.203‖	0.210
DBPC	C_{22}	348§	14.9§	15.0	—	0.240

*All properties are evaluated at $\pi = 50$ dyn/cm.
‡Mabrey and Sturtevant (1976).
§Phillips et al. (1969).
‖Nagle and Wilkinson (1978).

transitions in this latter case always proceed from a very closely packed configuration to one in which the area per molecule is very large. Indeed, near $\pi = 0$ the molecular area of the expanded phase turns out to be >1,000 Å^2/mol. This fact precludes fitting more than T_m to the experimental data at very low π. Thus, our results provide a model-based argument in favor of the larger value. Also, from Table II it is apparent that the enthalpy changes in the model are in good agreement with the observed values. We conclude that our model is a valid, semiempirically constructed description of the thermodynamic properties of pure lipid monolayers and bilayers. We now consider binary mixtures of lipid.

Binary Mixtures of Lipid

The phase diagrams we obtain for binary mxitures of $C_{14} - C_{16}$ and $C_{14} - C_{18}$ using the ideal mixing approximation are shown in Figs. 5 and 6, along with some of the data points of Mabrey and Sturtevant (1976). Agreement is fairly good for DMPC-DPPC mixtures, although the theoretical diagram is narrower than the experimental points. Experimental studies of DMPC-DSPC mixtures (Fig. 6) indicate a wide asymmetrical phase diagram that is not reproduced by the theoretical model. As we shall discuss later, this indicates a strong departure from ideal mixing due probably to chain mismatches. To examine the model for nonideal types of mixing we have constructed phase diagrams for DMPC-DSPC mixtures with both repulsive and attractive mixing energies of the form

$$E_{\text{mix}} = \frac{\pm \frac{1}{4}\left[C(14)X_{14} + C(18)X_{18}\right]}{(A\text{-}38)^{1.5}}. \tag{13}$$

The resulting phase diagrams are shown in Figs. 7 and 8. These plots are highly unsymmetrical, but the plot of Fig. 8, in which we use the "+" sign in Eq. 13 (a repulsive mixing interaction) shows the characteristics of the experimental "solidus" curve. One could consider different sorts of mixing energies other than Eq. 13, but we feel that choices are too arbitrary

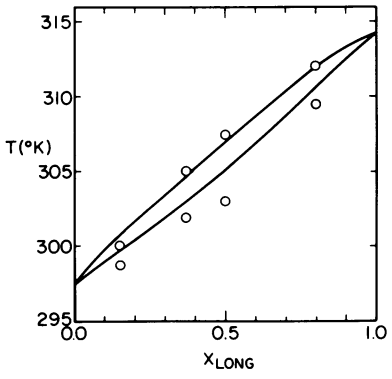

FIGURE 5

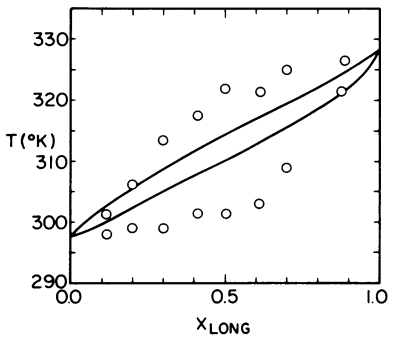

FIGURE 6

FIGURE 5 Temperature-composition phase diagram for DMPC-DPPC mixtures with ideal mixing. The solid curve is the theory result, while circles locate the data points of Mabrey and Sturtevant (1976).
FIGURE 6 Temperature-composition phase diagram for DMPC-DSPC mixtures with ideal mixing. Circles locate data points of Mabrey and Sturtevant (1976).

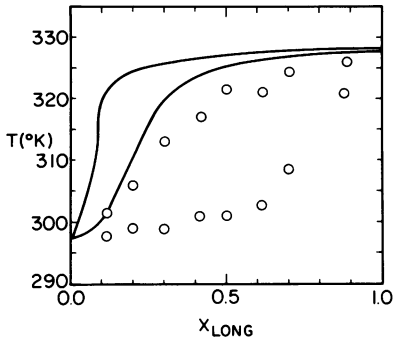

FIGURE 7

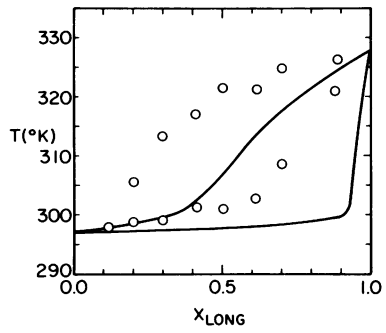

FIGURE 8

FIGURE 7 Temperature-composition phase diagram for DMPC-DSPC mixtures with an attractive mixing interaction; Eq. 13 with "−" sign. Circles are data points of Mabrey and Sturtevant (1976).
FIGURE 8 Temperature-composition phase diagram for DMPC-DSPC with a repulsive mixing interaction; Eq. 13 with a "+" sign. Circles are data points of Mabrey and Sturtevant (1976).

and against the semiempirical nature of our efforts. Figs. 5–8 illustrate types of phase diagrams one can expect with this model.

Lipid-Protein Mixtures

In Fig. 9, using $\pi - A$ isotherms, we show results of our studies of lipid-protein mixtures in our model. These isotherms are somewhat sensitive to the value of the area for the protein used in the attractive energy function, Eq. 12. If 105 Å^2 is chosen for this area, the value of the protein concentration, 0.12, at which the phase transition disappears, is in good agreement with the experimentally determined value at which the bilayer transitions, seen calorimetrically, disappear (Chapman et al. 1977), although lateral monolayer pressures are substantially raised. When we study the same lipid-protein mixture in bilayers at a fixed lateral pressure of 50 dyn/cm using the Gibbs free energy, we find that increasing protein concentration rapidly lowers the phase transition temperature by increasing the effective distance between lipids and thereby lowering the attractive potential energy. In our lipid-protein mixture calculations we have also monitored the effective lipid-mediated protein interaction (Marčelja, 1976):

$$V_p = (\partial G/\partial X_p), \tag{14}$$

where X_P is the protein concentration. We find that in all cases $V_P > 0$, indicating that the lipid-mediated force is repulsive in our model. The description of lipid-protein mixtures provided by this model thus seems accurate only if the lateral pressure is allowed to increase rapidly with increasing protein concentration. In the next section we discuss the consequences of our findings.

V. DISCUSSION

Single-Component Systems

The basic properties of the model presented in this paper are summarized in Tables I and II. Table II indicates that by adjusting the interaction parameter C we can fit many of the

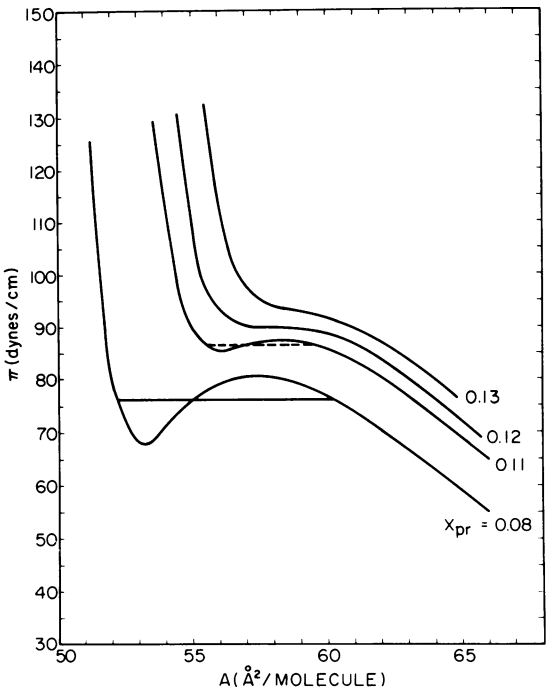

FIGURE 9 Pressure-area plots of DPPC-protein mixtures, all at T = 314°K, for varying protein concentration. The lipid phase transition disappears in a critical point at X_{pr} = 0.12, for the protein parameters given in the text.

experimental properties of the various bilayers quite closely. This implies that our methods of analyzing interchain packing and long-range interactions provide a good model for the actual systems. Analysis of the change in van der Waals energies at the transition, compared with experiment in Table II, points out that the semiempirical potential is well constructed for the description of single-component systems using scaled particle theory. Although scaled particle theory is inexact, it is very accurate for the description of hard-core systems, so that our use of this theory should provide an accurate model for systems more complex than those amenable to exact mathematical analysis (Nagle, 1973). Details of the very close packing at low temperatures, such as the symmetry of the frozen state, are, of course, beyond the scope of this treatment.

While the scaled particle treatment is fairly accurate and rigorous, we are still forced to choose a semiempirical potential (Eq. 7) to obtain the theoretical description of phase transitions. In making this choice we have attempted to follow experimental and theoretial guidelines when possible. Most importantly, we have not allowed any parameters other than C to vary from system to system. The potential in Eq. 8 is, therefore, to be considered as a mathematical approximation to the true intermolecular potential energy.

The choice of 50 dyn/cm as an effective lateral pressure for our system is also based upon indirect evidence and arguments. However, as we stated earlier, this value is used in all cases, so that it is not a fitting parameter. The success of the model (Table II) provides indirect support for π = 50 dyn/cm.

In Figs. 3 and 9 we have presented monolayer type $\pi - A$ data, obtained under the assumption that bilayer and monolayer phase transitions are the same phenomena viewed under different thermodynamic conditions of constraint. This property of the model is also evident when one compares Figs. 1 and 3. Fig. 1 is calculated at fixed pressure (Gibbs free energy minimized) and Fig. 3 at fixed areas (Helmholtz free energy minimized). In practice, problems such as monolayer solubility or solvent interactions may lead to differences between the two systems but, at least ideally, they appear to have the same properties. It should be pointed out that all model data are compared with experimental results for bilayers, so that the model is not compromised by any conclusions regarding monolayer stability or equilibration problems.

Binary Mixtures of Lipid

One of the major advantages of this model is that generalization from single-component systems to mixtures simply invovles mixing together a larger variety of cylinders. The phase diagrams are obtained by the double tangent construction illustrated in Fig. 4. Although the cylinder mixing is straightforward, the nature of the interaction between unlike lipids is not so simple to model within our semiempirical approach. For this reason we first chose to consider the simplest possibility, that of ideal mixing. Here the average van der Waals force experienced by a randomly selected molecule does not depend upon whether the molecule is type A or type B. Using this hypothesis we obtain the phase diagrams of Figs. 5 and 6, respectively. The calculated diagrams are narrow compared with the data of Mabrey and Sturtevant (1976), but the agreement for $C_{14} - C_{16}$ mixtures is reasonably good. The discrepancy in the $C_{14} - C_{18}$ mixtures (Fig 6) between theory and experiment suggests that nonideal mixing interactions are involved. Accordingly, we considered mixing interactions of the form of Eq. 13, and the results are shown in Figs. 7 and 8. These two figures illustrate the effect of mixing interactions on phase diagrams in this model, and were chosen for this purpose rather than for fitting experimental data. It is very difficult to estimate in our semiempirical approach the effect of mismatches in chain length upon the free energy.

Successful application of this model to binary lipid mixtures lies in its ability to describe theoretically phase separations without the introduction of additional adjustable parameters. The relatively successful description of $C_{16} - C_{14}$ mixtures indicates that our ideal mixing hypothesis can be trusted (since no other parameters or assumptions are involved) for this system. Chain mismatch contributions to E_{att} that violate the ideal mixing hypothesis are the most likely reason the description of $C_{14} - C_{18}$ mixtures is not as successful. Also, the fact that the van der Waals energy changes in the model are too large (Table II) for C_{18} means that mixtures involving this lipid are not as accurately described. Further improvements in theoretical descriptions of mixtures could involve changing the formula for the areas of the various states (Eq. 5) to allow for expansion, and somehow including interactions designed to simulate the effects of the chain mismatches.

Lipid-Protein Mixtures

We have studied the thermodynamic properties of lipid-protein mixture both in the $\pi - A$ plane and at fixed pressure. The effects of increased concentrations of protein at fixed temperature (Fig. 9) show that the lipid phase transition is shifted to higher pressures and the entropy change is reduced as the protein concentration increases until, at ~12% protein, the

transition disappears at a critical point. This reduction in the entropy change to zero at $X_P = 0.12$ is consistent with experimental data for gramicidin A-DPPC Bilayers (Chapman et al., 1977). When we study bilayers at 50 dyn/cm, however, we find that the transition temperature decreases rapidly with increasing protein concentration. This is not surprising, in light of the behavior of simpler systems in which impurities lower the melting temperature by partially impairing the onset of long-range order. Indeed, detailed examination of the model under these circumstances shows that, as protein content increases, the disorder in the lipid phase increases rather than decreases, as one might expect from boundary lipid considerations. This increase in disorder is due to the reduction in van der Waals attractive energy as the average interlipid distance increases. Thus, increased pressure is necessary to force the system to order. This might be remedied by introducing a protein-lipid van der Waals-like attractive energy. In the present model there is no such attraction, and the lipid-mediated interprotein force $\partial G/\partial X_P$ is always repulsive. In Marčelja's (1976) model this derivative is negative when an attractive lipid-protein force is included in the treatment. In the spirit of our semiempirical investigation we have not considered any additional parameter-dependent terms in the basic model at this stage.

We thank Professor J. P. Chandler for helpful discussions.

This research was supported in part by National Science Foundation grant PCM 76-20679.

Received for publication 1 March 1979 and in revised form 23 May 1979.

REFERENCES

ALDER, B., and T. WAINWRIGHT. 1960. Studies in molecular dynamics II. Behavior of a small number of elastic spheres. *J. Chem Phys.* **33**:1439–1450.

CHAPMAN, D., B. A. CORNELL, A. W. ELIASZ, and A. PERRY. 1977. Interactions of helical polypeptide segments which span the hydrocarbon region of lipid bilayers. Studies of the Gramicidin A lipid-water system. *J. Mol. Biol.* **113**:517–538.

CHENG, W. H. 1978. Theoretical Model for Lipid Phase Transitions and Phase Diagrams. Ph.D. Thesis, Oklahoma State University, Stillwater.

DEVAUS, P., and H. M. MCCONNELL. 1972. Lateral diffusion in spin-labeled phosphatidylcholine multibilayers. *J. Am. Chem. Soc.* **94**:4475–4481.

FRISCH, H. L., and LEBOWITZ, J. L., editors. 1964. The Equilibrium Theory of Classical Fluids. The Benjamin Co., Inc., New York. 299–302.

GERSHFELD, N. 1968. Cohesive forces in monomolecular films at an air-water interface. *Adv. Chem. Ser.* **84**:45–130.

HUI, S. W., M. COWDEN, D. PAPAHADJOPOULOS, D., and D. F. PARSONS. 1975. Electron diffraction of hydrated phospholipid single bilayers. *Biochim. Biophys. Acta.* **382**:265–274.

JACKSON, M. B. 1976. A β-coupled kink description of the lipid bilayer phase transition. *Biochemistry.* **15**:2555–2561.

JACOBS, R. E., B. HUDSON, and H. C. ANDERSEN. 1975. A theory of the chain melting transition of aqueons phospholipid dispersions. *Proc. Nat. Acad. Sci. U.S.A.* **72**:3993–3997.

JACOBS, R. E., B. HUDSON, and H. C. ANDERSEN. 1977. A theory of phase transitions in one- and two-component phospholipid bilayers. *Biochemistry.* **16**:4349–4359.

LEBOWITZ, J. L., E. HELFAND, and E. PRAESTGARD. 1965. Scaled particle theory of fluid mixtures. *J. Chem. Phys.* **43**:774–779.

MABREY, S., and J. M. STURTEVANT. 1976. Investigation of phase transitions of lipids and lipid mixtures by high sensitivity differential scanning calorimetry. *Proc. Nat. Acad. Sci. U.S.A.* **73**:3862–3866.

MARČELJA, S. 1974. Chain ordering in liquid crystals II. Structure of bilayer membranes. *Biochim. Biophys. Acta.* **367**:165–176.

MARČELJA, S. 1976. Lipid-mediated protein interaction in membranes. *Biochim. Biophys. Acta.* **455**:1–7.

McCAMMON, J. A., and J. M. DEUTCH. 1975. "Semiempirical" models for biomembrane phase transitions and phase separations. *J. Am. Chem. Soc.* **97**:6675–6681.

NAGLE, J. F. 1973. Theory of biomembrane phase transitions. *J. Chem. Phys.* **58**:252–264.

NAGLE, J. F. 1976. Theory of lipid monolayer and bilayer phase transitions. Effect of head group interactions. *J. Membr. Biol.* **27**:233–250.

NAGLE, J. F., and A. WILKINSON. 1978. Lecithin bilayers: density measurements and molecular interactions. *Biophys. J.* **23**:159–176.

PHILLIPS, M. C., R. M. WILLIAMS, and D. CHAPMAN. 1969. On the nature of hydrocarbon chain motions in lipid liquid crystals. *Chem. Phys. Lipids.* **3**:234–244.

SCOTT, H. L., JR. 1975. A theoretical model for lipid monolayer phase transitions. *Biochim. Biophys. Acta.* **406**:329–346.

SCOTT, H. L., and W. H. CHENG. 1977. Lipid monolayer phase transitions: theoretical considerations. *J. Colloid Interface Sci.* **62**:125–130.

SEELIG, J., and W. NIEDERBERGER. 1974. Two pictures of a lipid bilayer. A comparison between deuterium label and spin-label experiments. *Biochemistry.* **13**:1585–1588.

TARDIEU, A., V. LUZZATI, and F. C. REMAN. 1973. Structure and polymorphism of the hydrocarbon chains of lipids: a study of lecithin-water phases. *J. Mol. Biol.* **75**:711–733.